Protection of grid connected photovoltaic system during voltage sag

Majid Taghizadeh[1], Javad Sadeh[1] and Ebadollah Kamyab[1,2]

[1]Electrical Engineering Department Faculty of Engineering, Ferdowsi University of Mashhad, Mashhad, Iran
[2]Researcher Operation Department, Khorasan Regional Electric Company Mashhad, Iran

Abstract: The grid-connected power electronic inverters are highly sensitive to grid disturbances and it is important to emphasize the necessity to reduce the effects of voltage disturbances on their operation. Among the wide range of power quality disturbances, voltage sags severely affect the performance of voltage source converters (VSC) operation of distributed generation (DG) units. In this paper, small signal model of photovoltaic, DC-DC boost converter and inverter are simulated in Matlab simulink software. The photovoltaic system is connected to a 20kV distribution feeder via a transformer. It can be seen if the voltage sag is happened in the system, the inverter switch current will be increased significantly. In order to protect the power electronic converters' switches during a voltage sag and increase the voltage sag ride through capability, use of fault current limiter (FCL), is proposed. It is shown that if the voltage sag happened with duration of half to thirty cycles, FCL limits the current of power electronic switches. So, the photovoltaic system although is kept connecting with grid during the voltage sag condition, the power elec-tronic switches aren't harmed and have normal current during voltage sag duration.

Keywords: Grid connected photovoltaic, voltage sag, DC-DC converter, current control inverter, fault current limiter

1 Introduction

Renewable energy sources are gaining more and more interest in recent years due to the exploitation of oilfields and to political crises in some strategic areas of the world. photovoltaic distributed generations have dc output voltage, so they should connect to grid via power electronic converters.

The operation of power electronic interfaces during extreme voltage disturbance is harmful and can damage power electronic converters. One of the most common power frequency disturbances is voltage sag. Voltage sag is defined as a momentary decrease in the rms voltage, with a duration ranging from half a cycle up to one minute [l]. It is caused by fault conditions within the plant or power system and lasts until the fault is cleared by a fuse or breaker. On the utility side, the fault condition may be a result of lightning, storm, contamination of insulators, animals or accidents [2]. The problem of voltage sags is important because it can cause loss of production and revenue due to the tripping of equipment sensitive to voltage variations [3]. Operation of DG units under voltage sags has not received much attention in the past. The main reason is that many grid operators demand the immediate disconnection of DG in case of grid disturbances as prerequisite for service continuing. However, as the power generated by DG units increases, this behavior stresses the utility grid and could cause power unbalance, which may turn into instability. So, the interaction between DG units and the grid during voltage sag is very important and it must be considered. Base on DG technologies, voltage sag ride through capabili-ties control strategy is presented. For example in [4-6] analysis and control of wind turbine during voltage sag are analysis. In [7], a fuel cell (FC), is connected to grid and propose a control strategy with super capacitor technology to make FC connect to grid during voltage sag.

In this paper small signal model of photovoltaic, DC-DC boost converter and inverter is simulated in Matlab/Simulink software. In order to take maximum power from photovoltaic system a perturbation and observation (P&O) algorithm is use and the DC voltage link is control with this strategy that, if inverter can deliver all power from photovoltaic system to grid, the DC voltage link can fixed in a desire level with a PI controller.

The DC voltage level in this paper is 1000V and the grid voltage level is 380V phase to ground. The photovoltaic system is connected to a 20kV distribution feeder via a transformer. In this situation, voltage sag with different amplitude is happened in the system and as it is anticipated, the inverter current switches are increased significantly. In this paper in order to protect the power electronic switches during voltage sag and increase the voltage sag ride through capability, a fault current limiter (FCL) is used.

This paper has been organized as follows. In section II, a photovoltaic grid connected system is design. In section III, voltage sag types introduce and in section IV dynamic model of a super conductive fault current limiter (SFCL) is presented. The proposed technique is validated by simulations and the obtained results are discussed in section V, and finally, the conclusions are summarized in section VI.

2 Grid connected photovoltaic system

Design and small signal modeling of a

*Corresponding author (email: taghizdeh.majid@ieee.org; sadeh@ieee.org; ebadkamyab@yahoo.com)

978-1-4244-9620-4/11/$26.00 ©2011 IEEE

grid-connected photovoltaic (PV) system is a main part of voltage sag analysis, because the voltage sag duration is ranging from half a cycle up to one minute, so each part of the system should have a precise and accurate model to have a good judgment. In Figure 1 schematic diagram of a grid connected photovoltaic system is shown.

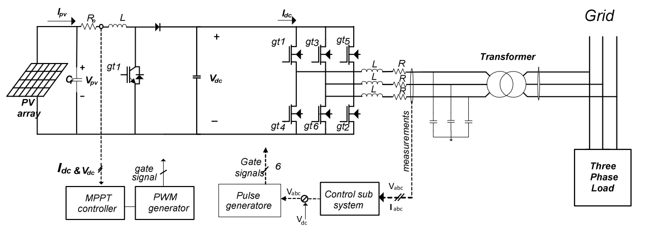

Figure 1 Grid connected photovoltaic system

In the first stage photovoltaic system is connected to a boost DC-DC converter. DC-DC converter rises the low solar voltage to a suitable level correspond to the optimal PV power. At the next stage a DC to AC inverter that operates in a current control mode supplies continuous power from dc link bus to three phase grid system. An output RLC filter is used to reduce the ripple due to PWM operation.

Modeling and control of each part of the system is presented as fallows.

2.1 PV model

Through the years, different circuit models have been used to study and simulate the behavior of a photovoltaic cell. A DC voltage source is the simplest method used for simulating the photovoltaic cells [8]. The problem with this method is that a photovoltaic cell does not behave completely as a dc voltage source. Another approach to simulate a photovoltaic cell, with an acceptable precision, is using the one diode model [9]. The problem with this model is that it requires information that is not easily found in a data sheet. In this paper, the model presented in [10] will be used which is a more practical PV cell model. The advantage of this model over the others relies in that all the parameters can be simply obtained in the manufacturer data sheet. Figure 2 shows the schematic diagram of a PV model. Details of this model is presented in [10] to calculate I_{PV}.

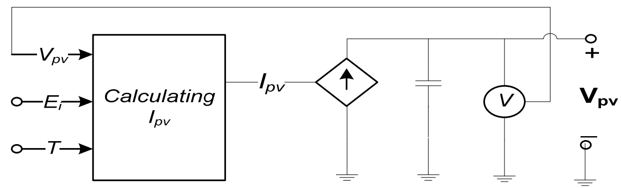

Figure 2 Photovoltaic model

2.2 DC-DC Boost Converter

As the PV output voltage changes during a day, because of different temperature and radiation, in order to meet a constant voltage at DC link, a DC-DC boost converter is used. The structure of DC-DC converter is shown in Figure 1. The maximum power point tracker (MPPT) is used to control the boost converter as shown in Figure 3. The P&O algorithm [11] is used to find the maximum power point of the PV system.

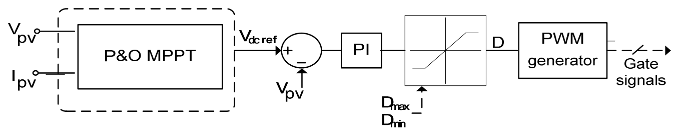

Figure 3 Control structure of boost converter and MPPT algorithm

2.3 Inverter

As shown in Figure 1 three phase voltage source inverter has six IGBTs and it is used to deliver dc power from dc link to ac grid side. In order to do this it should design a controller to establish gate signal for IGBTs. Schematic diagram of the inverter controller in current mode control is shown in Figure 4.

To establish gate signals, it is needed to transfer voltage and current of grid to rotating axis with equation 1.

$$\begin{bmatrix} f_d \\ f_q \\ f_0 \end{bmatrix} = C \begin{bmatrix} f_a \\ f_b \\ f_c \end{bmatrix} \quad C = \frac{2}{3}\begin{bmatrix} \sin(\omega t) & \sin(\omega t - 2\pi/3) & \sin(\omega t + 2\pi/3) \\ \cos(\omega t) & \cos(\omega t - 2\pi/3) & \cos(\omega t + 2\pi/3) \\ \frac{1}{2} & \frac{1}{2} & \frac{1}{2} \end{bmatrix} \tag{1}$$

In (1) f is voltage and current signals and ω is angular frequency. Network reference current expressed in d-q frame, are given by (2) [12]. P and Q are reference active and reactive powers. v_d and v_q are grid voltage at d-q refrence.

$$\begin{bmatrix} i_d^* \\ i_q^* \end{bmatrix} = \frac{1}{v_d^2 + v_q^2} \begin{bmatrix} P^* & -Q^* \\ Q^* & P^* \end{bmatrix} \begin{bmatrix} v_d \\ v_q \end{bmatrix} \tag{2}$$

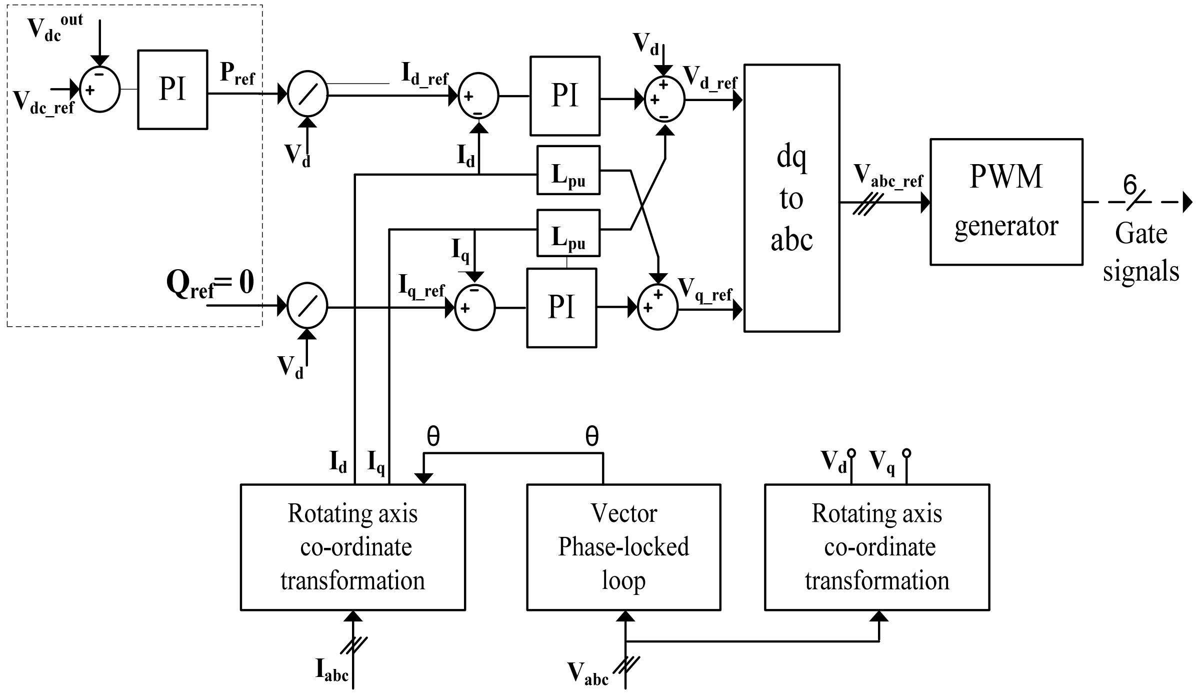

Figure 4 Current mode control of three phase inverter

With equation (2) the inverter always delivers a fixed power to ac grid system, but in grid connected PV system power is not fixed and it changes during day. In order to takes this into account, in Figure 4, diagram of controller is modified and shown in the dashed part of Figure 4. This control strategy makes inverter to deliver all power generated from PV to grid and control the dc link voltage at desire level.

3 Voltage sag characteristic

Voltage sag is defined as a immediate decrease in the rms voltage, with a duration ranging from half a cycle up to one minute. It has a negative impact in voltage source converters used in adjustable-speed drives, grid connected photovoltaic system, industrial processes control and full-scale wind turbines, leading undesirable tripping on their protection devices. Voltage sags creation are generally caused by over loading, induction motors starting procedures and grid faults. Regarding the operation of grid connected VSI, the voltage sag characteristics of interest are the magnitude, the duration and the phase-angle jump. The voltage sags due to grid faults can be classified in seven different types [13].

The type A is the results from balanced three-phase short-circuits. The other six types are the results from unbalanced faults. For example, phase-to-ground (type B), phase-to-phase (type E) and the two-phase-to-ground (type C). The remaining types result from the propagation of these unbalanced faults through $\Delta - Y$ connected transformers.

4 Dynamic model of a super-conductive fault current limiter (SFCL)

Basically FCL is a variable impedance that is installed in series with a circuit breaker. In the fault situations, the impedance rises to a value at which the fault current is reduced to a lower level that the circuit breaker can with-stand it. Many kinds of fault current limiting devices have been moved forward in accordance with the development of power electronics, magnet technologies and super conducting materials [14]–[17]. In this paper, high temperature resistive superconducting fault current limiters is used [18]. The most important physical property for the current limiting behaviors of the SFCL is the E~J characteristic of the High Temperature Superconductors (HTS) and its dependence on temperature T.

E~J characteristic can be divided into three sub-regions: superconducting state, flux flow state and normal conducting state. Each region is approximated by an exponential power law. This parameterization holds generally for all high temperature superconducting materials. Together with the thermal–diffusion equation, it forms the basis for the simulation of the high temperature SFCL [19].

Relation between E~J is correspond to the supercon-ducting state. In superconducting state E is zero and in flux flow state and normal conducting state, can be evaluated by (3) and (4):

$$E = E_c(\frac{J}{J_c})^{n(T)} \qquad J > J_c \ , \ T < T_c \qquad (3)$$

$$E = \rho(T_c)(\frac{T}{T_c}).J \qquad J > J_c \ , \ T > T_c \qquad (4)$$

In these equations E_c is critical field, J_c is critical current density, T_c is critical temperature, E is electrical filed, J is current density, T is temperature and ρ is specific resistivity in normal state.

So with being E by (3) and (4) and knowing current density, temperature of the superconducting is computed using (5).

$$C\frac{dT}{dt} = E(J,T).J(t) \qquad (5)$$

where C is the heat capacity per volume. So, the specific resistivity of the superconducting in each temperature is calculated using (6) and (7) [16].

$$\rho_r = (\frac{E_c}{J_c}).(\frac{J}{J_c(T)})^{n-1} \qquad T < T_c \qquad (6)$$

$$\rho_r = (\frac{E_c}{J_c}).(\frac{T}{T_c}) \qquad T > T_c \qquad (7)$$

n is a value around 10. So, resistivity of a superconducting material with length L and cross section A is shown in (8).

$$\rho = \rho_r(\frac{L}{A}) \qquad (8)$$

5 Simulation and results

In order to protect a grid connected photovoltaic system during voltage sag, a 20kV distribution feeder as shown in Figure 5 with a 315kW PV system connected to grid via power electronic switch is simulated in Matlab software. In Figure 6, detailed structure of photovoltaic system that is simulated in Matlab software is shown.

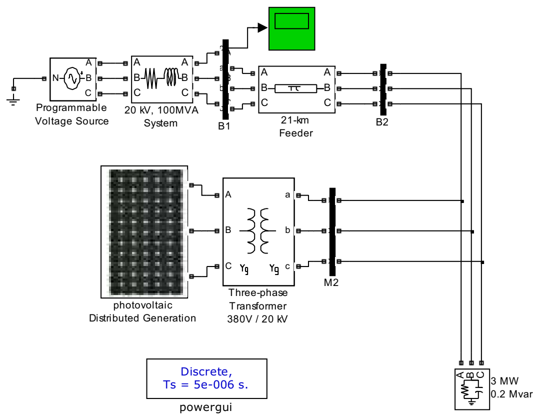

Figure 5 System under study

System and PV distributed generation parameters are listed in Table 1.

Table 1 *Parameters of the system*

PV Rated Power	315 kW	Frequency	50 Hz
PV Rated Voltage	619 V	Phase to phase grid voltage (HV)	20 kV
DC voltage Link	1000 V	Phase to phase grid voltage (LV)	380 V
DC Capacitor	6000 µF	Feeder length	21 km
Temperature	$25\,^{o}$ C	Sample Time	5e-6
Radiation	1000 W/m^2	Inverter frequency Pulse	3850 Hz
R Filter	0.01 Ω	Boost frequency pulse	10 kHz
L Filter	0.0001 H	DG transformer connection	Y_g-Y_g
C Filter	1e(-10) F	Load	(3+0.2i) MVA

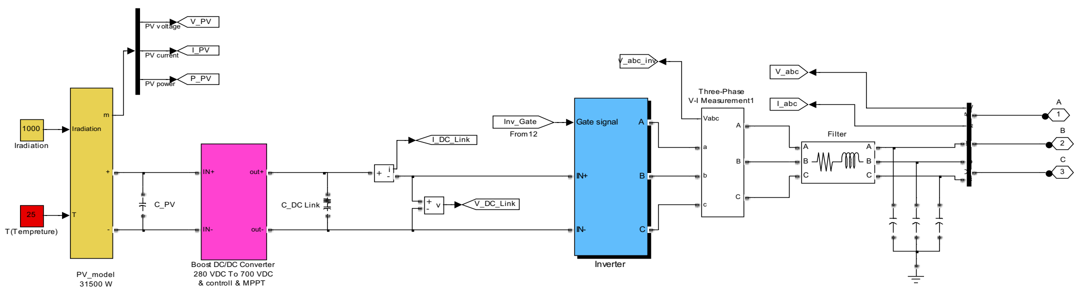

Figure 6 Photovoltaic grid connected system in details

At first, the system is in normal state and photovoltaic system is delivered its maximum power to the grid. In Figure 7 PV power, PV voltage and PV current are shown. Voltage and current of inverter are shown in Figure 8 and the active and reactive power of inverter are depicted in Figure 9.

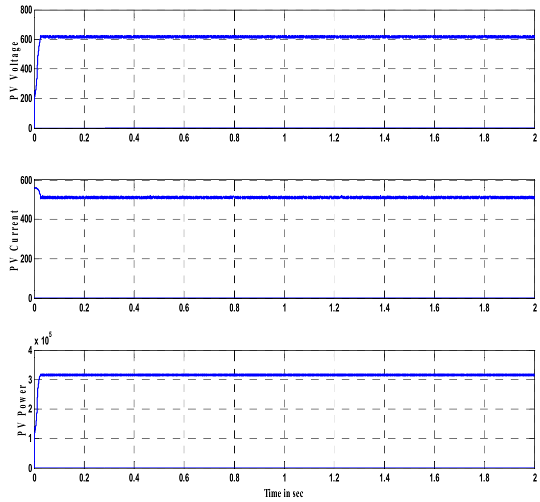

Figure 7 Voltage, current and power of photovoltaic sytem

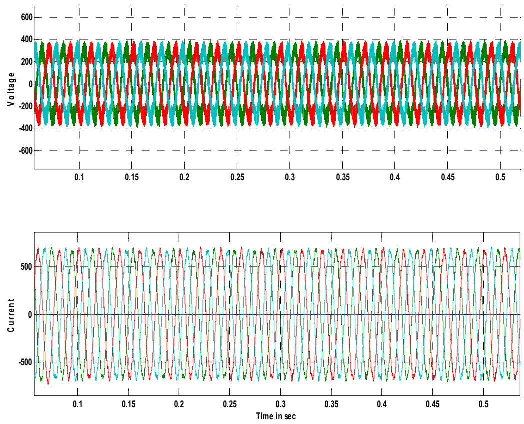

Figure 8 Inverter voltage and current

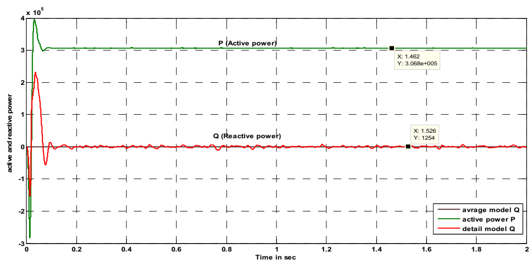

Figure 9 Active and reactive power of Inverter

As mentioned previously, inverter has 6 power electronic switches and the full capacity of inverter switches are used. The current of one of inverter switches is shown in Figure 10 when the system is in normal condition.

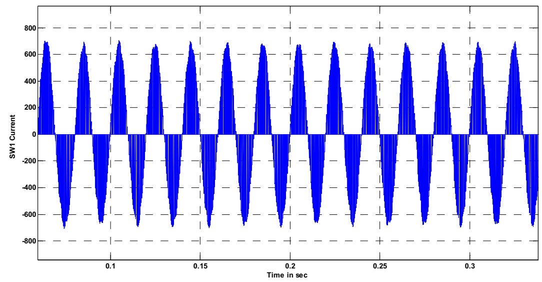

Figure 10 Phase A inverter switch Current

Now let assume a single phase to ground fault occur at the grid. So a voltage sag which decreases the phase A voltage is happened and it remains for ten cycles. As shown in Fig-ure 11, in this situation, the PV power feed to grid is approximately constant. Because the voltage in DC link is not drop, so the current of inverter switches are increased significantly as shown in Figure 12. In this situation, the distributed PV generation system is disconnected, in order to protect the inverter switches from over load and harms.

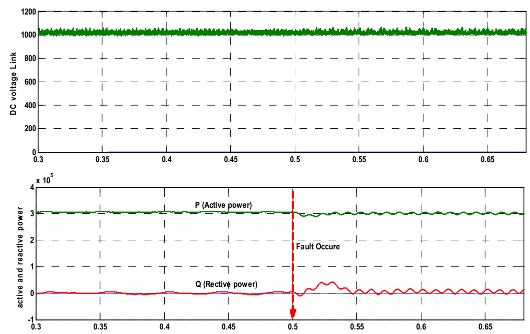

Figure 11 DC voltage link, active and reactive power during voltage sag

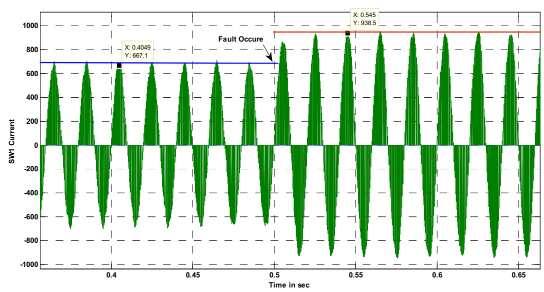

Figure 12 Phase A inverter switch current during voltage sag

However, as the power generated by DG units increases, this behavior stresses the utility grid and could cause power unbalance, which may turn into instability. In order to protect the distributed PV generation during voltage sags, in this paper SFCL is used after DG transformer in the common coupling point. In Figures 13 and 14, it is shown that in voltage sag condition, although the system connect to grid, current of inverter switches are in normal ranges and the injected power to grid is nominal value. Figure 15 shows the temperature and resistance of SFCL during the voltage sag condition.

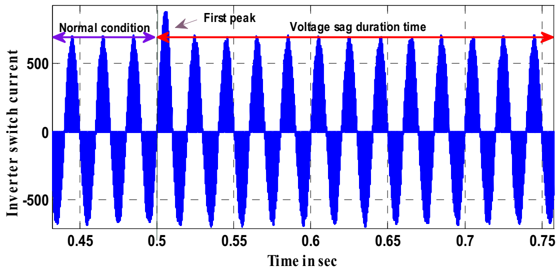

Figure 13 Phase A inverter switch current during voltage sag with SFCL

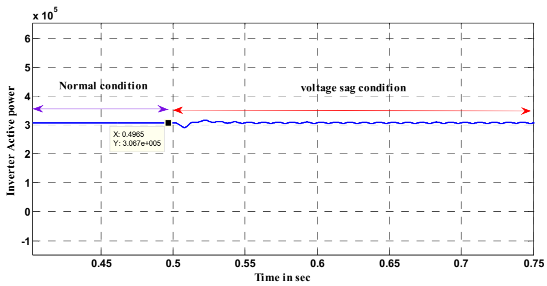

Figure 14 Photovoltaic injected power during voltage sag

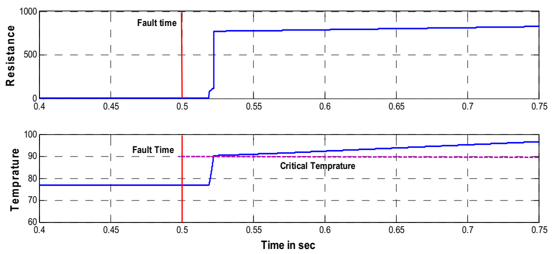

Figure 15 Resistance and temperature of SFCL during sag

6 Conclusion

In this paper a grid connected PV distributed generation is simulated in normal condition and during voltage sag situation. It is shown that if a fault occurred in the system it results in voltage sag in the system and also at the common coupling point where the PV system is connected. During voltage sag the output power injected to grid from PV system is approximately constant or drop a little, and at the same time, the DC voltage link is also constant and those result in the current of inverter switches increase until voltage sag disappear. In order to protect PV distributed generation from voltage sag in this paper using a SFCL is proposed and it is shown that during voltage sags, PV system can still connect to grid and deliver power to grid, without damage to inverter switches from fault over-current.

1 M.H. Bollen, " Understanding power quality problems: voltage sags and interruptions", New York, IEEE Press,1999.

2 IEEE Recommended Practice for Monitoring Electric Power Quality, IEEE Std. 1159-1995, June 1995.

3 M. McGranaghan, D. Mueller, and M. Samotyj, "Voltage Sags in Industrial System," Transactions on Industry Applications, vol. 29, no. 2, March-April 1993.

4 Y. Zhou, P. Bauer, A. Ferreira and J. Pierik, "Operation of grid-connected DFIG under unbalanced grid voltage condition," IEEE Transactions Energy Conversion, vol. 24, no. 1, pp. 240–246, March 2009.

5 D.S. Martin, J.L.R. Amenedo and S. Arnaltes, "Providing ride-through capability to a doubly fed induction generator under unbalanced voltage dips," IEEE Trans. Power Electron., vol. 24, no.7, pp. 1747-1775, July 2009.

6 M. H. J. Bollen, G. Olguin, and M. Martins, "Voltage dips at the terminals of wind power installations," Wind Energy, vol. 8, no. 3, pp. 307–318, Jul. 2005.

7 A. Hajizadeh and M.A. Golkar, "Fuzzy neural control of a hybrid fuel cell/battery distributed power generation system", IET Renewable Power Generation, December 2009-Vol. 3, Issue 4, p. 402–414.

8 C. Liuchen and N. Cecilia, "A Solar Battery Charger with improved energy utilization". Canadian Conference on Electrical and Computer Engineering, vol. 1, pp. 105-108, 25-28 Sep 1994

9 S. Kim, M.B. Kim and M.J. Youn, "New maximum power point tracker using sliding-mode observer for estimation of solar array current in the grid- connected photovoltaic system" IEEE Transactions on Industrial Electronics, Vol 53, No.4, August 2006, Page(s): 1027

10 O. Rivera, I. Eduardo and F.Z. Peng, "Analytical model for a photovoltaic module using the electrical characteristics provided by the manufacturer sheet", PESC'05. IEE 36th vol. Page(s):2087-2091, 11-14 Sept.2005

11 S. Jain and V. Agarwal, "A New Algorithm for Rapid Tracking of Approximate Maximum Power Point in Photovoltaic Systems," IEEE Power Electronic Letter., Vol. 2, pp. 16-19, Mar. 2004.

12 N. Hamrouni, M. Jraidi, A. Cherif and A. Dhouib " Modeling, simulation and control of PV pumping system ", In EIEctrMACS 05, Hammemet, Tunisia, 2005

13 M.H.J. Bollen and L.D. Zhang," Different methods for classification of three-phase unbalanced voltage dips due to faults," Science Direct Renewable Energy, ELSEVIER, pp. 59–69, July 2003.

14 R.F. Gieseetal, "Assessment study of super conducting fault current limiter soperation at 77K," IEEE Transactions on Power Delivery, vol. 8, no. 3, pp. 1138–1147, July 1993.

15 R.K. Smithetal, "Solid state distribution current limiter and circuit breaker application requirements and control strategies," IEEETransactions on Power Delivery, vol. 8, no. 3, pp. 1155–1164, July 1993.

16 E. Thurieseta, "Toward the superconducting fault current limiter," IEEE Transactions on Power Delivery, vol. 6, pp. 801–808, April 1991.

17 M. Chenetal, " Fabrication and characterization of superconducting Rings for fault current limiter application," IEEE Transaction on Applied Superconductivity, vol. 282–287, pp. 2639–2642, 1997.

18 L.Y. Klaus and P. Juengst, "Modeling and simulation of high temperature resistive superconducting fault current limiters " IEEE transactions on Applied Superconductivity, vol. 14, no. 2, June 2004.

19 W. Paul and M. Chen, "Superconducting fault current limiter applications, technical & economical benefits and simulations & test results," in 13-201CIGRE, Session-2000, Paris, France, pp.1–8.